This Accepted Manuscript has not been copyedited and formatted. The final version may differ from this version.

JNeurosci
THE JOURNAL OF NEUROSCIENCE

Research Articles: Neurobiology of Disease

Activity-dependent dysfunction in visual and olfactory sensory systems in mouse models of Down syndrome.

Christopher M. William[1], Lubna Saqran[3], Matthew A. Stern[3], Charles L. Chiang[3], Scott Herrick[3], Aziz Rangwala[3], Mark W. Albers[3], Matthew P. Frosch[2,3] and Bradley T. Hyman[3]

[1]*New York University Medical School, Department of Pathology, 550 First Avenue, New York, NY 10016.*
[2]*Neuropathology Service*
[3]*MassGeneral Institute for Neurodegenerative Disease, Neurology, Massachusetts General Hospital, 114 16th St., Charlestown, MA 02129*

DOI: 10.1523/JNEUROSCI.1045-17.2017

Received: 18 April 2017

Revised: 8 August 2017

Accepted: 5 September 2017

Published: 12 September 2017

Author contributions: C.M.W., L.S., M.A.S., S.P.H., M.W.A., M.P.F., and B.T.H. designed research; C.M.W., L.S., M.A.S., C.L.C., S.P.H., and A.R. performed research; C.M.W., L.S., M.A.S., C.L.C., and S.P.H. analyzed data; C.M.W., M.A.S., S.P.H., M.W.A., and B.T.H. wrote the paper.

Conflict of Interest: The authors declare no competing financial interests.

This work was supported by NIH (K08 NS069811 and a pilot project grant from 5P50AG005134 to C.M.W; 5P50AG005134 to BTH; R21NS085711 and R21NS094861 to M.W.A.). We thank Natalia Garcia de Marco for advice on Somatostatin immunohistochemistry. We thank members of the Hyman and Albers labs for advice and discussion.

Corresponding author: Christopher M. William MD PhD, New York University Medical School, Department of Pathology, TH 387, 560 First Avenue, New York, NY 10016, Work: 646-501-0689, Fax: 212-263-7916, christopher.william@nyumc.org

Cite as: J. Neurosci ; 10.1523/JNEUROSCI.1045-17.2017

Alerts: Sign up at www.jneurosci.org/cgi/alerts to receive customized email alerts when the fully formatted version of this article is published.

Accepted manuscripts are peer-reviewed but have not been through the copyediting, formatting, or proofreading process.

Copyright © 2017 the authors

JNeurosci Accepted Manuscript

JNeurosci Accepted Manuscript

Activity-dependent dysfunction in visual and olfactory sensory systems in mouse models of Down syndrome.

Abbreviated title: Early plasticity and connectivity defects in Down syndrome model mice

Christopher M. William[1], Lubna Saqran[3], Matthew A. Stern[3], Charles L. Chiang[3], Scott Herrick[3], Aziz Rangwala[3], Mark W. Albers[3], Matthew P. Frosch[2,3] and Bradley T. Hyman[3]

[1]New York University Medical School, Department of Pathology, 550 First Avenue, New York, NY 10016. [2]Neuropathology Service, [3]MassGeneral Institute for Neurodegenerative Disease, Neurology, Massachusetts General Hospital, 114 16th St., Charlestown, MA 02129

Corresponding author: Christopher M. William MD PhD, New York University Medical School, Department of Pathology, TH 387, 560 First Avenue, New York, NY 10016
Work: 646-501-0689
Fax: 212-263-7916
christopher.william@nyumc.org

Number of pages: 23

Number of Figures: 6

Number of words: Abstract: 250; Significance statement: 117; Introduction: 503; Discussion: 1287

Acknowledgements: This work was supported by NIH (K08 NS069811 and a pilot project grant from 5P50AG005134 to C.M.W; 5P50AG005134 to BTH; R21NS085711 and R21NS094861 to M.W.A.). We thank Natalia Garcia de Marco for advice on Somatostatin immunohistochemistry. We thank members of the Hyman and Albers labs for advice and discussion.

Conflict of interest: The authors declare no competing conflict of interest.

JNeurosci Accepted Manuscript

Significance Statement: Our understanding of the basis for intellectual impairment in Down syndrome is hindered by the large number of genes duplicated in Trisomy 21 and a lack of understanding of the effect of disease pathology on the function of neural circuits *in vivo*. This work describes early postnatal developmental abnormalities in visual and olfactory sensory systems in Down syndrome model mice which provide insight into defects in the function of neural circuits *in vivo* and provide an approach to explore the genetic and molecular basis for impairment in the disease. In addition, these findings raise the possibility that basic dysfunction in primary sensory circuitry may illustrate mechanisms important for global learning and cognitive impairment in Down syndrome patients.

Abstract

Activity-dependent synaptic plasticity plays a critical role in the refinement of circuitry during postnatal development and may be disrupted in conditions that cause intellectual disability such as Down syndrome (DS). To test this hypothesis, visual cortical plasticity was assessed in Ts65Dn mice that harbor a chromosomal duplication syntenic to human chromosome 21q. We find that Ts65Dn mice demonstrate a defect in ocular dominance plasticity (ODP) following monocular deprivation. This phenotype is similar to that of transgenic mice that express amyloid precursor protein (APP), which is duplicated in DS and in Ts65DN mice; however, normalizing APP gene copy number in Ts65Dn mice fails to rescue plasticity. Ts1Rhr mice harbor a duplication of the telomeric third of the Ts65Dn-duplicated sequence and demonstrate the same ODP defect, suggesting a gene or genes sufficient to drive the phenotype are located in that smaller duplication. In addition, we find that Ts65Dn mice demonstrate an abnormality in olfactory system connectivity, a defect in the refinement of connections to second-order neurons in the olfactory bulb. Ts1Rhr mice do not demonstrate a defect in glomerular refinement, suggesting that distinct genes or sets of genes underlie visual and olfactory system phenotypes. Importantly, these data suggest that developmental plasticity and connectivity are impaired in sensory systems

JNeurosci Accepted Manuscript

in DS model mice, that such defects may contribute to functional impairment in DS, and that these phenotypes, present in male and female mice, provide novel means by which to examine the genetic and molecular bases for neurodevelopmental impairment in model mice *in vivo*.

Introduction

Down syndrome (DS) patients experience profound delay in the attainment of developmental milestones as well as impairment in multiple cognitive domains including speech, language production and short term memory (reviewed by Chapman and Hesketh, 2000). To better understand the physiologic and molecular bases for these phenotypes, mouse models of Down syndrome have been generated. Down syndrome model mice that harbor duplications of mouse sequence syntenic to human chromosome 21 (Olson et al., 2007; Pereira et al., 2009; Reeves et al., 1995; Sago et al., 1998; Yu et al., 2010) or that carry an independently segregating copy of human chromosome 21 (O'Doherty et al., 2005) demonstrate learning and behavioral abnormalities suggesting that some aspects of human impairment may be modeled in mice. The genetic bases for these phenotypes, the effects of gene dosage dysregulation on the function of intact circuits *in vivo* and whether postnatal functional deficits are the result of in utero developmental abnormalities or are exacerbated by ongoing gene dysregulation throughout life are all issues critical to the design of therapeutic strategies to prevent or reverse cognitive impairment in DS.

Little is known about the function of the DS model cortex during early postnatal development, when neural activity sculpts cortical connectivity. We hypothesize that the dysregulation of gene expression caused by trisomy 21 may impair early cortical plasticity and contribute to functional impairment of the cerebral cortex in DS. To assess circuit-level plasticity in DS model mice *in vivo*, we have taken advantage of two well-characterized forms of plasticity in the visual and olfactory systems. We find that Ts65Dn DS model mice demonstrate a defect in visual cortical plasticity, ocular dominance plasticity (ODP). Our previous work suggested that overexpression

JNeurosci Accepted Manuscript

of amyloid precursor protein (APP) and amyloid beta are sufficient to cause impairment of critical period ODP in mouse models of Alzheimer's disease (William et al., 2012), leading to the hypothesis that overexpression of APP in the trisomy 21 model might contribute to plasticity defects. Surprisingly, however, we find that rescuing APP trisomy in Ts65Dn mice by breeding a null allele of APP into the line, restoring the number of copies of APP to 2N, does not prevent ODP impairment in those mice, suggesting that other duplicated genes are likely sufficient to drive the phenotype in Ts65Dn mice. We have also found that the Ts1Rhr DS model strain, harboring a duplication containing approximately 33 genes (excluding APP) in what has been termed the Down syndrome critical region, demonstrates the same plasticity defect, reinforcing the conclusion that the plasticity defect is not dependent on triplication of the APP locus.

In addition, we have found that Ts65Dn mice demonstrate impairment in the refinement of synaptic connections by olfactory neurons in the olfactory bulb. Further genetic dissection suggests that APP gene dosage does not drive the phenotype, nor is the Ts1Rhr duplication sufficient to reproduce the defect. These data reveal the possibility of multiple chromosome 21-linked, activity-dependent abnormalities in sensory system plasticity and connectivity that may contribute to the extent of cognitive impairment in DS patients.

Materials and Methods

Mouse strains. Mice with segmental trisomy for chromosome 16 (Ts65Dn; B6EiC3Sn a/A-Ts(17<16>65Dn/J; strain 005252, Jackson laboratory), mice with a duplication of a smaller portion of the sequence duplicated in the Ts65Dn line (*Ts1Rhr* mice; B6.129S6-Dp(16Cbr1-Fam3b)1Rhr/J; gift of William Mobley; strain 005383, Jackson laboratory, maintained on a C57BL/6 and C3H hybrid background for comparison with Ts65Dn mice) and their non-trisomic litter mates were studied in these experiments (Olson et al., 2007; Reeves et al., 1995). In addition, mice heterozygous for APP ($APP^{+/-}$ mice; B6.129S7-Apptm1Dbo/J; strain 004133, Jackson laboratory) were obtained from Jackson laboratory and bred with Ts65Dn mice to

JNeurosci Accepted Manuscript

produce Ts65Dn; $APP^{+/-}$ mice (Ts65Dn; APP2N mice; Zheng et al., 1995). Animal experiments were performed in accordance with United States National Institutes of Health guidelines and were approved by the Institutional Animal Care and Use Committees of Massachusetts General Hospital.

Surgery. Monocular deprivation (MD), via unilateral lid suture, was performed on P27-P29 transgenic and non-transgenic mice, with lid reopening and *Arc* induction, as described in William et al. (2012), 4-6 days after MD. For optical imaging studies, P23-P25 mice underwent reinforced thin skull preparation with headpost implantation. Reinforced thin skull preparation was performed as described in Drew et al. (2010). Following recovery from surgery and restraint training, mice underwent pre-MD optical imaging and contralateral lid suture (MD) at P27-29. After 6 days, the sutured lid was reopened and post-MD imaging performed. All surgeries and subsequent analyses were performed blind to genotype.

Arc induction. Adapted from Tagawa *et al*. (2005). The eye opposite the one to be stimulated was removed the day prior to *Arc* induction. Mice were then placed in a ventilated, dark chamber for 15 hours and exposed to light, 30 minutes for *Arc* mRNA induction or 2 hours for Arc protein induction.

Arc in situ hybridization and quantification. *In situ* hybridization was performed as described in William et al. (2012). Briefly, in situ hybridization with an *Arc* antisense probe was performed on 10 μm, coronal, primary visual cortical sections. The visual cortex ipsilateral to the stimulated eye is photographed and a rectangle is drawn across layer 2/3 of the *Arc*-positive domain for quantitation of *Arc* domain width. A plot profile is generated along the long axis of the rectangle, parallel to the cortical surface, averaging staining intensity across the short axis and the width of the *Arc*-positive domain is calculated as the full width at half maximum (FWHM). Averages of staining intensity medial to the *Arc*-positive domain and within the area of greatest staining intensity are used to determine the value for half maximum above background. 5 or more

JNeurosci Accepted Manuscript

sections were used in the quantitation of responses per mouse. Image analysis is performed in FIJI (NIH).

Immunohistochemistry, WFA staining and cell counting. Immunohistochemical and Wisteria Floribunda agglutinin (WFA; see below) stains were performed on coronal sections of the brains of 6 Ts65Dn trisomic and 6 non-trisomic littermate mice that underwent 2-hour Arc induction, to facilitate subsequent labeling of lateral visual cortex using Arc immunohistochemistry, followed by PBS cardiac perfusion, immersion fixation in 4% paraformaldehyde for 24 hours and embedding in OCT (23-730-571, Fisher Scientific). 10 μm coronal sections through the posterior brain were serially collected on 10 slides with 200 μm of distance between each series of sections every 100 μm and serially distributed across 10 slides. Sections were stained by overnight incubation with guinea pig anti-Arc (Cat# 156 005, Synaptic Systems; 1:1000), mouse anti-NeuN (MAB377, Millipore; 1:1000), mouse anti-Parvalbumin (P3088, Sigma; 1:4000), rabbit anti-Somatostatin (ab64053, Abcam; 1:1000), and mouse anti-Gad67 (MAB5406, Millipore; 1:1000) antibodies and/or WFA (FL-1351, Vector Laboratories; 1:1000) after 10 minute post fixation with 4% PFA, permeabilization with 0.3% Tween-20 and blocking with 10% goat serum. WFA-stained slides were coverslipped using Slowfade mounting medium without glycerol (S-2828, ThermoFisher). All other slides were mounted using Vectashield with DAPI (H-1200, Vector Laboratories).

The portion of each coronal section that contained visual cortex was determined by costaining for Arc or comparison to a serial section stained for Arc in which the outline of the Arc-positive and medial monocular visual cortex were outlined using CAST software (Olympus) to then allow measuring of the area counted as well as the number of cells within each area. For NeuN counts, 30% of the analyzed area was sampled in an unbiased, stereologic approach using the CAST system.

Olfactory glomerular refinement assay. As described in Cao et al. (2012), we examined the precision of olfactory sensory neuron (OSN) axon targeting in Ts65Dn, Ts65Dn;APP2N, Ts1Rhr,

JNeurosci Accepted Manuscript

and non-trisomic mice with ages ranging from P34-P45. To visualize the OSN axonal projection patterns, we immunostained the olfactory bulbs from these mice with antibodies against the M71 and MOR28 olfactory receptors (ORs). The numbers of glomeruli receiving either M71 or MOR28 receptor neuron projections per half bulb were quantified for each mouse.

Immunohistochemistry of olfactory bulb glomerular refinement assay. As described in Cao et al. (2012), the olfactory bulbs (OBs) of Ts65Dn and Ts1Rhr mice were immunostained using antibodies against the M71 and MOR28 olfactory receptors (ORs; Barnea et al., 2004). The olfactory bulbs were dissected, embedded in M1 (1310TS; ThermoFisher Scientific) and frozen in a dry ice/ethanol bath. Twenty µm slices of the OB were cryosectioned and collected on SuperFrost Plus slides (12-550-15, Fisher Scientific). Sections were post-fixed with 4% paraformaldehyde in PBS for 8 minutes at room temperature, washed three times in PBS for 10 minutes, permeabilized in 0.1% Triton X-100 in PBS (PT) for 30 minutes. at room temperature, blocked in 5% heat-inactivated donkey serum in PT (PTS) for 1 hour at room temperature, and incubated with primary antibody (rabbit anti-MOR28, 1:3000; guinea pig anti-M71, 1:1000; Barnea et al., 2004) in PTS under a Hybrislip (H18202; ThermoFisher Scientific) overnight in a humidified chamber at 4°C. The following day, sections were washed three times with PT for 10 minutes, blocked with PTS for 30 minutes at room temperature, incubated with a fluorescent-conjugated secondary antibody (Cy3-conjugated donkey anti-guinea pig IgG, Jackson Immunoresearch, 1:500) in PTS for 2 hours at room temperature, washed briefly in PBS, and coverslipped with Fluoromount G with DAPI (0100-20; Southern Biotech). Slides were imaged using a Zeiss inverted fluorescent microscope and analyzed using FIJI (NIH).

Optical imaging of intrinsic signals. Mice are presented with an upward drifting grating (0.03 cycles/degree, 2 Hz) occupying a 16° area of the visual field to the right of the vertical midline, 20° above the horizontal meridian. Stimulus was presented to left or right eye for 5 seconds, followed

JNeurosci Accepted Manuscript

by 20 seconds of blank screen at mean luminance. For a detailed description of imaging parameters and analysis, please see William et al (2012).

Experimental design and statistical analysis: *Pde6b* genotyping was performed to ensure that experimental mice did not harbor *rd1* mutations due to the C3H component of the mixed background in which all mice were maintained. Littermate control mice are used in all experiments for comparison with trisomic Ts65Dn or Ts1Rhr mice. Male (n=101) and female (n=65) mice were used in the experiments described in this study and the gender composition of study arms was similar in each experiment. Two-tailed Student's t-tests and two-way ANOVAs were calculated as described in the text using StatView (Version 5.0.1; SAS Institute Incorporated).

Results

Critical period visual cortical plasticity defects in Ts65Dn mice

To test whether DS model mice demonstrate defects in cortical plasticity during early postnatal development, ocular dominance plasticity was assessed in one of the best-characterized mouse models of DS, the Ts65Dn line, which harbors a large duplication of mouse chromosome 16 that is syntenic to the majority of human chromosome 21q (Reeves et al., 1995). Ocular dominance plasticity can be triggered in the primary visual cortex by a brief loss of vision in one eye via lid suture (monocular deprivation, MD) that results in several changes in the subsequent responsiveness of the visual cortex to stimulation of each eye: expansion of the area of the visual cortex that responds to the non-deprived eye (ipsilateral to the non-deprived eye), weakening of responses to stimulation of the deprived eye and strengthening of responses to stimulation of the non-deprived eye (Gordon and Stryker, 1996; Tagawa et al., 2005). The cortical response to monocular challenge is most robust during a critical period at one month of age (Gordon and Stryker, 1996), during which all of the following studies were performed. Two complementary approaches were used to measure cortical responses following MD, induction of the immediate

JNeurosci Accepted Manuscript

early gene *Arc* to label the visual cortex responsive to the non-deprived eye and optical imaging of intrinsic signals to measure the strength of cortical responses to stimulation of each eye.

A brief period of visual stimulation induces *Arc* expression in many responding excitatory neurons in the visual cortex, highlighting the binocular visual cortex ipsilateral to the stimulated eye (Figure 1 A-D; Tagawa et al., 2005). In normally-reared mice, the pattern and width of the responsive domains of visual cortex are similar in Ts65Dn and control mice (width of *Arc*-positive domain in non-trisomic cortex, 871 ± 56 μm, n=6; width in Ts65Dn cortex, 879 ± 32 μm, n=6 mice; p=0.14, t-test; Figure 1A and 1B). Following a period of 4-6 days of MD, stimulation of the non-deprived eye reveals an expansion in the area of the visual cortex responsive to that eye, indicating a normal plastic response in control mice (width post-MD, 1108 ± 69 μm, n=14 mice; $p=7.75 \times 10^{-7}$, t-test; Figure 1C and E). This expansion is not seen in Ts65Dn mice (874 ± 80 μm, n=7; p=0.95, t-test; Figure 1D and E). A significant interaction exists between genotype and MD ($p<0.0001$; two-way ANOVA), confirming that Ts65Dn mice do not demonstrate the normal plastic response to MD. To assess whether the abnormality that we observe in critical period plasticity in Ts65Dn mice is caused by a delay in the timing of the critical period, we have tested plasticity following a 6-day period of MD in 2-3 month-old Ts65Dn mice and find a similar defect (non-trisomic width of *Arc*-positive domain post-MD, 1041 ± 7 μm, n=2; Ts65Dn width, 801 ± 51 μm, n= 4 mice; p=0.003, t-test).

Intrinsic imaging is an alternative assay to measure visual cortical responses *in vivo*. We first assessed whether a primary defect in vision might underlie the observed difference in critical period plasticity. Ts65Dn mice demonstrate responses of comparable magnitude to those of control mice (Figure 2B) and the width of the peak of response at half of the maximum value is similar in non-trisomic and Ts65Dn mice (non-trisomic width at half-maximum, 934 ± 279 μm, n=6; Ts65Dn width at half maximum, 866 ± 130 μm, n=7; p=0.29, t-test), suggesting similar responsiveness of Ts65Dn cortex to visual stimulation. Following a 6-day period of MD, non-

JNeurosci Accepted Manuscript

trisomic mice demonstrate weakening of responses to the deprived eye, contralateral to the imaged cortex, and strengthening of responses to the ipsilateral, non-deprived eye (Figure 2B, black bars, Pre- and Post-MD). Following MD, Ts65Dn mice demonstrate weakening of responses to the deprived eye, however, they fail to demonstrate strengthening of responses to the non-deprived eye (Figure 2B; red bars, Pre- and Post-MD). As a result, the shift in ocular dominance that is observed in non-trisomic mice is not as robust in Ts65Dn mice (Figures 2C and D). A significant interaction is present between genotype and shift in ocular dominance index (ODI) post-MD (non-trisomic ODI pre-MD, 0.186 ± 0.030, n=8; post-MD, -0.312 ± 0.080, n=8; Ts65Dn ODI pre-MD, 0.117 ± 0.047, n=10; post-MD, -0.038 ± 0.057, n=6; p=0.0058, two-way ANOVA), consistent with a defect in OD plasticity in Ts65Dn mice.

Histologic evaluation of visual cortex in Down syndrome model mice

Several groups have reported abnormalities in neurogenesis involving excitatory and inhibitory neurons in Down syndrome (DS) model mice (Chakrabarti et al., 2010; Chakrabarti et al., 2007; Haydar and Reeves, 2012; Perez-Cremades et al., 2010); to assess whether significant defects in the generation of cortical neurons are present in the visual cortex and may contribute to the defect in plasticity that we observe in Ts65Dn mice, we performed immunohistologic analysis of P28-32 trisomic and littermate control mice. We observe no significant difference in the thickness of the visual cortex in Ts65Dn and control mice (non-trisomic cortical thickness, 1,479 ± 83 μm, n=6; Ts65Dn cortical thickness, 1,428 ± 32 μm, n=6; p=0.19, t-test). The density of $NeuN^+$ neurons is similar in non-trisomic and Ts65Dn visual cortex (non-trisomic $NeuN^+$ neuronal density, 2,380 ± 324 neurons/mm^2, n=6; Ts65Dn density, 2115 ± 556 neurons/mm^2; p=0.34, t-test; Figure 3A-C). We see comparable numbers of $Gad67^+$ inhibitory neurons (non-trisomic $Gad67^+$ neuronal density, 117.4 ± 32.3 neurons/mm^2, n=6; Ts65Dn density, 123.1 ± 23.5 neurons/mm2, n=6; p= 0.73, t-test; Figure 3D-F) in Ts65Dn and non-trisomic mice and comparable numbers of parvalbumin-expressing (non-trisomic $parvalbumin^+$ neuronal density, 102 ± 36 neurons/mm^2,

JNeurosci Accepted Manuscript

n=6; Ts65Dn density, 103 ± 39 neurons/mm^2, n=6; p=0.99, t-test; Figure 3G-I) and somatostatin-expressing inhibitory neuronal subtypes (non-trisomic somatostatin+ neuronal density, 33.3 ± 7.7 neurons/mm^2, n=6; Ts65Dn density, 32.1 ± 6.8 neurons/mm^2, n=6; p=0.39, t-test; Figure 3J-L) in non-trisomic and Ts65Dn mice. Similarly, we find no significant difference in the number of inhibitory neurons enshrouded in perineuronal nets (PNNs; non-trisomic density of PNNs, 82.5 ± 30.8 neurons/mm^2, n=6; Ts65Dn density, 71.9 ± 11.1 neurons/mm^2, n=6; p=0.29, t-test), a-chondroitin sulfate proteoglycan-rich extracellular matrix which matures during the critical period and aids in inhibition of plasticity after the critical period (Pizzorusso et al., 2002; Ye and Miao, 2013). These data suggest that the plasticity impairment that we observe in Ts65Dn mice cannot be easily attributed to a significant decrease in the number of neurons, an abnormality in the number of inhibitory neurons or by aberrant or delayed maturation of PNN matrix in the primary visual cortex.

APP-duplication does not drive the OD plasticity defect in Ts65Dn mice

We had previously demonstrated that expression of a mutant allele of the amyloid precursor protein (APP) gene was sufficient to block critical period OD plasticity in transgenic mice (William et al., 2012), and Ts65Dn mice have been demonstrated to overexpress APP (Reeves et al., 1995), raising the possibility that overexpression of APP and its proteolytic cleavage product, amyloid-beta (Aβ), may be responsible for the plasticity impairment that we observe in Ts65Dn mice. To test this hypothesis, a mutant allele of APP was crossed into the Ts65Dn strain and Ts65Dn mice heterozygous for the endogenous APP locus (Ts65Dn; APP2N) mice were assessed for their ability to exhibit OD plasticity. Following a 6-day period of MD, Ts65Dn; APP2N mice fail to demonstrate an expansion in the domain of visual cortex responsive to the non-deprived eye (width of *Arc*-positive visual cortex ipsilateral to the non-deprived eye, 866 ± 37 μm, n=7). Moreover, no strengthening of responses to non-deprived eye stimulation is observed following 6 days of MD (pre-MD response to non-deprived eye stimulation, 0.49 ± 0.05%; post-MD

JNeurosci Accepted Manuscript

response, 0.46 ± 0.04%, n=12; p=0.2, t-test; Figure 4A). A significant, but modest decline in ODI is observed in Ts65Dn; APP2N mice (pre-MD ODI, 0.22 ± 0.04; post-MD ODI, -0.03 ± 0.07; p=0.007, t-test; Figure 4B) driven entirely by weakening of responses to the deprived eye (pre-MD response to deprived eye stimulation, 0.74 ± 0.04%; post-MD response, 0.43 ± 0.05%, n=11; $p=6.03 \times 10^{-5}$, t-test; Figure 4A). These data are a phenocopy of the results obtained in Ts65Dn mice and they suggest that duplication of the APP gene is not required to drive OD plasticity impairment in Ts65Dn mice.

The Down syndrome critical region is sufficient to drive OD plasticity impairment

To begin to define a minimal region within the Ts65Dn duplication sufficient to cause visual system plasticity impairment, OD plasticity was assessed in the Ts1Rhr mouse line that harbors a duplication roughly one-third of the size of that of the Ts65Dn line (Olson et al., 2007). The sequence included in this duplication corresponds to a region of human chromosome 21 that has been termed the "Down syndrome critical region" due to its ability to confer a number of Down syndrome-associated phenotypes when duplicated in patients with partial duplications of chromosome 21 (Rahmani et al., 1989). In the absence of a challenge, Ts1Rhr mice and non-trisomic littermates demonstrate similar patterns of *Arc* expression upon stimulation of the ipsilateral eye (non-trisomic Arc^+ domain width, 870 ± 25 μm, n=6; Ts1Rhr domain width, 898 ± 42 μm, n=5; p=0.21, t-test; Figure 5 A, B and E). Following a 6-day period of MD, however, Ts1Rhr mice demonstrate a defect in the plastic expansion in cortex responsive to the non-deprived eye as assessed by *Arc* expression (post-MD non-trisomic Arc^+ domain width, 1156 ± 72 μm, n=9; compared to normally-reared, $p= 4.4 \times 10^{-7}$, t-test; post-MD Ts1Rhr domain width, 899 ± 52 μm, n=9; compared to normally-reared p=0.97, t-test; Figure 5 C-E). A significant interaction is present between genotype and deprivation (p<0.0001, two way ANOVA). Ts1Rhr mice demonstrate robust responses that are comparable to those of non-trisomic mice (Figure 5A), with similar response widths (non-trisomic full width at half maximum (FWHM) of response to

JNeurosci Accepted Manuscript

contralateral eye stimulation, 665 ± 162 μm, n=6; Ts1Rhr FWHM, 691 ± 202 μm, n=6; p=0.8, t-test). Following a challenge of 6 days of MD, non-trisomic mice demonstrate weakening of responses to the deprived eye (contra) and strengthening of responses to the non-deprived eye (ipsi; black bars Pre- and Post-MD; Figure 5F). Ts1Rhr mice demonstrate weakening of responses to the deprived eye following deprivation, but also demonstrate weakening of responses to the non-deprived eye (pre-MD non-deprived eye dF/F, 0.74 ± 0.04%; post-MD dF/F, 0.58 ± 0.04%; p=0.02, t-test; red bars Pre- and Post-MD, Figure 5F). The shifts in ODI that occur in non-trisomic mice are less robust in Ts1Rhr mice and a significant interaction is observed between genotype and challenge (p=0.024, two-way ANOVA; Figure 5 G and H). These data indicate that Ts1Rhr mice demonstrate a defect in OD plasticity similar to that of Ts65Dn mice, an inability of the visual cortex to strengthen responses to stimulation of the non-deprived eye following the loss of input from the contralateral eye.

Olfactory glomerular target refinement is disrupted in DS model mice.

The plasticity impairments observed in the visual systems of Ts65Dn and Ts1Rhr mice raised the possibility that plasticity in other sensory systems may be perturbed in DS model mice. During early postnatal development, the synapses between olfactory sensory neurons (OSNs) in the olfactory epithelium and tufted and mitral cells in the olfactory bulb undergo activity–dependent refinement (Zou et al., 2004). The synapses between OSNs and second order neurons in the bulb are organized into discrete spheres of neuropil, termed glomeruli, such that OSNs that express the same odorant receptor all synapse within the same glomerulus (Mombaerts et al., 1996; Vassar et al., 1994). In the mature bulb, the axon projections of OSNs expressing a given odorant receptor converge on a single glomerulus in each half of the olfactory bulb. Through a process that requires OSN activity, refinement of connections to a single glomerulus per hemibulb occurs (Yu et al., 2004). A critical window exists during which OSN activity is required for refinement to occur (Ma et al., 2014; Tsai and Barnea, 2014; Zou et al., 2004). For example,

JNeurosci Accepted Manuscript

OSNs expressing the odorant receptor M71 demonstrate an activity-dependent window that closes by postnatal day 25 (Zou et al., 2004), suggesting that by P34, much of this refinement has already occurred. To assess glomerular refinement in the olfactory system, the distal projections of M71-expressing neurons were labelled in the olfactory bulbs of Ts65Dn mice and non-trisomic littermates using an antibody to M71 (Barnea et al., 2004). Non-trisomic mice demonstrated 1-2 glomeruli targeted by M71 neurons (average number of glomeruli per hemibulb, 1.36 ± 0.13, n=14 foci; Figure 6A and C); this is expected as M71 glomerular refinement continues until P60-90 in wild type mice (Zou et al., 2004). Ts65Dn mice, however, exhibit a larger number of M71-targeted glomeruli per hemibulb (average number of glomeruli per hemibulb, 1.81 ± 0.12, n=26 foci; p=0.027, t-test; Figure 6B and C). Refinement of projections of neurons expressing the odorant receptor MOR28 to single glomeruli occurs normally in Ts65Dn mice (number of glomeruli per non-trisomic hemibulb, 1.0 ± 0.0, n=10 hemibulbs from 4 mice; number of glomeruli per Ts65Dn hemibulb, 1.0 ± 0.0, n=10 hemibulbs from 5 mice), suggesting that this population of olfactory sensory neurons is less sensitive to perturbation than the population expressing M71. Consistent with our visual system plasticity data, Ts65Dn;APP2N mice demonstrate a defect in M71 receptor glomerular refinement (average glomeruli per hemibulb, 1.77 ± 0.17 , n=13 hemibulbs from 4 mice; p=0.86 compared to Ts65Dn mice, t-test; Figure 6C), suggesting the connectivity abnormality observed in the olfactory systems of Ts65Dn mice is not driven by duplication of APP alone. Surprisingly, the smaller duplication present in Ts1Rhr mice does not appear to be sufficient to cause impairment of refinement of glomerular connectivity (average number of glomeruli per hemibulb in non-trisomic bulbs, 1.29 ± 0.16, n=14 hemibulbs ; average number of glomeruli per Ts1Rhr hemibulb, 1.39 ± 0.16, n=18 hemibulbs; p=0.66, t-test; Figure 6D-F), suggesting either that the neural system sensitivity to a plasticity-disrupting genetic landscape differs between olfactory and visual cortices, or that duplicated genes present outside of the Ts1Rhr duplication, but included in the Ts65Dn duplication, are required to cause this defect in refinement of OSN connections.

JNeurosci Accepted Manuscript

Discussion

To explore the possibility that defects in synaptic plasticity during early postnatal development may contribute to functional impairment in Down syndrome, we assessed critical period visual cortical plasticity in two mouse models of Down syndrome, the Ts65Dn and Ts1Rhr strains. Both demonstrate impairment in ocular dominance plasticity. The specific component of the plastic response that is impaired in these mice is the ability of the cortex to strengthen responses to the non-deprived eye following a 4-6 day period of contralateral lid closure, evidenced also as a lack of expansion in the proportion of the visual cortex that responds to the non-deprived eye.

Ts65Dn and Ts1Rhr mice demonstrate robust responses to visual stimulation in the absence of challenge and appropriate weakening of responses to the deprived eye following challenge, suggesting that many aspects of visual circuit function are intact in these mice. Blank et al. have described a retinogeniculate refinement abnormality in Ts65Dn and Ts1Rhr mice in which, prior to eye opening, trisomic mice demonstrate excessive refinement of contralateral and ipsilateral projections from each eye to target dorsal lateral geniculate nuclei (2011). Ts65Dn mice demonstrate normal retinal wave activity, suggesting that the phenotype was not secondary to altered retinal physiology (Blank et al., 2011). The impact of a retinogeniculate refinement phenotype on the cortical plastic response is not clear, though this data suggest that abnormalities are present at multiple levels along the visual circuit.

Another possible explanation for an impairment in the cortical plastic response lies in abnormalities in cortical development. Using markers of differentiated neurons, inhibitory neurons, subtypes of inhibitory neurons and a marker of inhibitory circuit maturation, we find no significant differences when comparing Ts65Dn and non-trisomic visual cortex. Abnormalities in neurogenesis and in inhibitory neuron numbers have been reported in the adult somatosensory cortex of Ts65Dn mice (Chakrabarti et al., 2010; Perez-Cremades et al., 2010). Those differences were not identified in the critical period-age visual cortex in our study; whether defects

JNeurosci Accepted Manuscript

in neurogenesis are more apparent at different ages in different cortical areas may be borne out of studies that more specifically address this question in the future.

Transgenic overexpression of mutant alleles of APP can impair critical period OD plasticity in mouse models of Alzheimer's disease (Maya-Vetencourt et al., 2014; William et al., 2012), raising the possibility that overexpression of wild type APP in Ts65Dn mice may contribute to the impairment observed in developmental plasticity. APP overexpression causes degeneration of basal forebrain cholinergic neurons in adult Ts65Dn mice (Salehi et al., 2006), but whether APP overexpression contributes to impairment at an earlier age is less clear. Two lines of evidence argue against a role for trisomy of APP in the ocular dominance plasticity phenotype present in Ts65Dn mice. Removing one functional allele of APP in Ts65Dn mice or studying mice with a smaller duplication of sequence that excludes the APP locus, we find that APP is not necessary to drive either visual or olfactory system phenotypes that we observe in Ts65Dn mice. Overexpression of wild-type murine APP via duplication of the endogenous locus would be expected to exert a milder effect on the organism than exogenous expression of the mutant human gene, though 2-fold increases in the concentration of wild type, murine Aβ have been demonstrated to impair hippocampal synaptic plasticity in vitro (Abramov et al., 2009). Another possibility is that the effect of duplication of murine APP on OD plasticity may be masked by the effects of duplication of other genes. Trisomy of murine APP may contribute to the defects that we observe, however, overexpression of other genes included in the Ts65Dn duplication appears to be sufficient to drive impairment in OD plasticity and olfactory glomerular refinement.

The finding that the Ts1Rhr sequence duplication is sufficient to cause a defect in cortical plasticity narrows down the list of possible genes responsible for the phenotype to a group of approximately 33 candidates. Overexpression of one gene duplicated in the Ts1Rhr sequence, dual-specificity tyrosine-phosphorylated and –regulated kinase 1A, DYRK1A, has been implicated in neurogenesis (Guedj et al., 2012), hippocampal plasticity impairment in vitro and in learning

JNeurosci Accepted Manuscript

and memory impairment in transgenic mice *in vivo* (Garcia-Cerro et al., 2014). Over expression of DYRK1A can produce cognitive impairment in mice (Branchi et al., 2004). Detailed dissection of the sequence duplicated in Ts1Rhr mice implicates the DYRK1A gene as contributing to neural system impairment in model mice, though DYRK1A duplication does not account for the entire phenotype in either Ts65Dn or Ts1Rhr mice (Garcia-Cerro et al., 2014; Jiang et al., 2015). Overexpression of DSCAM can phenocopy the excessive refinement of retinogeniculate connections observed in Ts1Rhr mice, though restoring the number of DSCAM genes to 2N in Ts1Rhr mice fails to rescue the phenotype (Blank et al., 2011). Therefore, DYRK1A, APP and DSCAM overexpression each cause defects in plasticity, but reducing them individually to 2N in the context of a larger trisomy does not rescue impairment, suggesting complex gene-gene interactions. Thus, the ocular plasticity phenotype and olfactory plasticity phenotype explored here, and the cognitive phenotypes previously described in Ts1Rhr mice (Belichenko et al., 2009), suggest a complicated picture in which multiple genes may be involved. A more detailed understanding of the effects of gene dosage on visual system plasticity will provide insight into the basis for dysfunction across circuits required for higher cognitive functions.

Ts65Dn mice demonstrate a defect in refinement of OSN projections onto single olfactory bulb glomeruli. This process has been demonstrated to require olfactory sensory neuron activity as it can be impaired by nares closure (Zou et al., 2004). The refinement defect present in Ts65Dn mice is less severe than that described in mice subjected to nares closure, suggesting that trisomy in this model does not completely impair activity-dependent target refinement. Whether the refinement defect that we observe persists into adulthood is an important question that will need to be pursued with additional time points in older mice. The underlying genetic cause of this phenotype may overlap with the activity-dependent impairment we observe in the visual cortex, though the abatement of this phenotype in Ts1Rhr mice suggests that additional or different genes contribute to the glomerular refinement defect in Ts65Dn mice (Table 1). Reduction of

JNeurosci Accepted Manuscript

APP copy number to 2N in Ts65Dn mice failed to rescue plasticity in the visual system or to rescue glomerular refinement in the olfactory bulb. Wild type human APP does not have the same ability to disrupt glomerular refinement as human APPswe when expressed in OSNs (Cao et al., 2012), which is consistent with our data suggesting that other genes drive the olfactory system phenotype in Ts65Dn mice. Thus the current data revealing marked defects in developmental plasticity in both olfactory and visual systems suggest that refinement of connectivity and plasticity is impaired across circuits throughout the nervous system in the developing Down syndrome brain.

Down syndrome patients demonstrate abnormalities in visual function secondary to refractive errors, strabismus, lens opacities and other defects (van Splunder et al., 2003); visual function may be further impaired by defects in activity-dependent plasticity in the visual cortex. Reduced spine density and dendritic arborization abnormalities have been described in the visual cortex of DS infants (Takashima et al., 1981), structural findings which may also be secondary to defects in the functional wiring of the visual system. A recent study revealed significant olfactory deficits in DS patients, even in a group of younger adults (ages 18-29; Cecchini et al., 2016). Patients with visual and hearing deficits have higher rates of intellectual disability (Maatta et al., 2006), suggesting that abnormalities in sensory circuits could contribute to learning impairment and cognitive development. Our data provide a model system to test the molecular underpinnings of these sensory defects, and to potentially provide a testbed for future behavioral or therapeutic interventions.

JNeurosci Accepted Manuscript

References

Abramov, E., Dolev, I., Fogel, H., Ciccotosto, G.D., Ruff, E., and Slutsky, I. (2009). Amyloid-beta as a positive endogenous regulator of release probability at hippocampal synapses. Nat Neurosci *12*, 1567-1576.

Barnea, G., O'Donnell, S., Mancia, F., Sun, X., Nemes, A., Mendelsohn, M., and Axel, R. (2004). Odorant receptors on axon termini in the brain. Science *304*, 1468.

Belichenko, N.P., Belichenko, P.V., Kleschevnikov, A.M., Salehi, A., Reeves, R.H., and Mobley, W.C. (2009). The "Down syndrome critical region" is sufficient in the mouse model to confer behavioral, neurophysiological, and synaptic phenotypes characteristic of Down syndrome. J Neurosci *29*, 5938-5948.

Blank, M., Fuerst, P.G., Stevens, B., Nouri, N., Kirkby, L., Warrier, D., Barres, B.A., Feller, M.B., Huberman, A.D., Burgess, R.W.*, et al.* (2011). The Down syndrome critical region regulates retinogeniculate refinement. J Neurosci *31*, 5764-5776.

Branchi, I., Bichler, Z., Minghetti, L., Delabar, J.M., Malchiodi-Albedi, F., Gonzalez, M.C., Chettouh, Z., Nicolini, A., Chabert, C., Smith, D.J.*, et al.* (2004). Transgenic mouse in vivo library of human Down syndrome critical region 1: association between DYRK1A overexpression, brain development abnormalities, and cell cycle protein alteration. J Neuropathol Exp Neurol *63*, 429-440.

Cao, L., Schrank, B.R., Rodriguez, S., Benz, E.G., Moulia, T.W., Rickenbacher, G.T., Gomez, A.C., Levites, Y., Edwards, S.R., Golde, T.E.*, et al.* (2012). Abeta alters the connectivity of olfactory neurons in the absence of amyloid plaques in vivo. Nat Commun *3*, 1009.

Cecchini, M.P., Viviani, D., Sandri, M., Hahner, A., Hummel, T., and Zancanaro, C. (2016). Olfaction in People with Down Syndrome: A Comprehensive Assessment across Four Decades of Age. PLoS One *11*, e0146486.

Chakrabarti, L., Best, T.K., Cramer, N.P., Carney, R.S., Isaac, J.T., Galdzicki, Z., and Haydar, T.F. (2010). Olig1 and Olig2 triplication causes developmental brain defects in Down syndrome. Nat Neurosci *13*, 927-934.

Chakrabarti, L., Galdzicki, Z., and Haydar, T.F. (2007). Defects in embryonic neurogenesis and initial synapse formation in the forebrain of the Ts65Dn mouse model of Down syndrome. J Neurosci *27*, 11483-11495.

Chapman, R.S., and Hesketh, L.J. (2000). Behavioral phenotype of individuals with Down syndrome. Ment Retard Dev Disabil Res Rev *6*, 84-95.

Drew, P.J., Shih, A.Y., Driscoll, J.D., Knutsen, P.M., Blinder, P., Davalos, D., Akassoglou, K., Tsai, P.S., and Kleinfeld, D. (2010). Chronic optical access through a polished and reinforced thinned skull. Nat Methods *7*, 981-984.

Garcia-Cerro, S., Martinez, P., Vidal, V., Corrales, A., Florez, J., Vidal, R., Rueda, N., Arbones, M.L., and Martinez-Cue, C. (2014). Overexpression of Dyrk1A is implicated in several cognitive, electrophysiological and neuromorphological alterations found in a mouse model of Down syndrome. PLoS One *9*, e106572.

Gordon, J.A., and Stryker, M.P. (1996). Experience-dependent plasticity of binocular responses in the primary visual cortex of the mouse. J Neurosci *16*, 3274-3286.

Guedj, F., Pereira, P.L., Najas, S., Barallobre, M.J., Chabert, C., Souchet, B., Sebrie, C., Verney, C., Herault, Y., Arbones, M.*, et al.* (2012). DYRK1A: a master regulatory protein controlling brain growth. Neurobiol Dis *46*, 190-203.

JNeurosci Accepted Manuscript

494 Haydar, T.F., and Reeves, R.H. (2012). Trisomy 21 and early brain development. Trends Neurosci *35*, 81-
495 91.
496 Jiang, X., Liu, C., Yu, T., Zhang, L., Meng, K., Xing, Z., Belichenko, P.V., Kleschevnikov, A.M., Pao, A.,
497 Peresie, J.*, et al.* (2015). Genetic dissection of the Down syndrome critical region. Hum Mol Genet *24*,
498 6540-6551.
499 Ma, L., Wu, Y., Qiu, Q., Scheerer, H., Moran, A., and Yu, C.R. (2014). A developmental switch of axon
500 targeting in the continuously regenerating mouse olfactory system. Science *344*, 194-197.
501 Maatta, T., Kaski, M., Taanila, A., Keinanen-Kiukaanniemi, S., and Iivanainen, M. (2006). Sensory
502 impairments and health concerns related to the degree of intellectual disability in people with Down
503 syndrome. Downs Syndr Res Pract *11*, 78-83.
504 Maya-Vetencourt, J.F., Carucci, N.M., Capsoni, S., and Cattaneo, A. (2014). Amyloid plaque-independent
505 deficit of early postnatal visual cortical plasticity in the 5XFAD transgenic model of Alzheimer's disease. J
506 Alzheimers Dis *42*, 103-107.
507 Mombaerts, P., Wang, F., Dulac, C., Chao, S.K., Nemes, A., Mendelsohn, M., Edmondson, J., and Axel, R.
508 (1996). Visualizing an olfactory sensory map. Cell *87*, 675-686.
509 O'Doherty, A., Ruf, S., Mulligan, C., Hildreth, V., Errington, M.L., Cooke, S., Sesay, A., Modino, S., Vanes,
510 L., Hernandez, D.*, et al.* (2005). An aneuploid mouse strain carrying human chromosome 21 with Down
511 syndrome phenotypes. Science *309*, 2033-2037.
512 Olson, L.E., Roper, R.J., Sengstaken, C.L., Peterson, E.A., Aquino, V., Galdzicki, Z., Siarey, R., Pletnikov, M.,
513 Moran, T.H., and Reeves, R.H. (2007). Trisomy for the Down syndrome 'critical region' is necessary but
514 not sufficient for brain phenotypes of trisomic mice. Hum Mol Genet *16*, 774-782.
515 Pereira, P.L., Magnol, L., Sahun, I., Brault, V., Duchon, A., Prandini, P., Gruart, A., Bizot, J.C., Chadefaux-
516 Vekemans, B., Deutsch, S.*, et al.* (2009). A new mouse model for the trisomy of the Abcg1-U2af1 region
517 reveals the complexity of the combinatorial genetic code of down syndrome. Hum Mol Genet *18*, 4756-
518 4769.
519 Perez-Cremades, D., Hernandez, S., Blasco-Ibanez, J.M., Crespo, C., Nacher, J., and Varea, E. (2010).
520 Alteration of inhibitory circuits in the somatosensory cortex of Ts65Dn mice, a model for Down's
521 syndrome. J Neural Transm *117*, 445-455.
522 Pizzorusso, T., Medini, P., Berardi, N., Chierzi, S., Fawcett, J.W., and Maffei, L. (2002). Reactivation of
523 ocular dominance plasticity in the adult visual cortex. Science *298*, 1248-1251.
524 Rahmani, Z., Blouin, J.L., Creau-Goldberg, N., Watkins, P.C., Mattei, J.F., Poissonnier, M., Prieur, M.,
525 Chettouh, Z., Nicole, A., Aurias, A.*, et al.* (1989). Critical role of the D21S55 region on chromosome 21 in
526 the pathogenesis of Down syndrome. Proc Natl Acad Sci U S A *86*, 5958-5962.
527 Reeves, R.H., Irving, N.G., Moran, T.H., Wohn, A., Kitt, C., Sisodia, S.S., Schmidt, C., Bronson, R.T., and
528 Davisson, M.T. (1995). A mouse model for Down syndrome exhibits learning and behaviour deficits. Nat
529 Genet *11*, 177-184.
530 Sago, H., Carlson, E.J., Smith, D.J., Kilbridge, J., Rubin, E.M., Mobley, W.C., Epstein, C.J., and Huang, T.T.
531 (1998). Ts1Cje, a partial trisomy 16 mouse model for Down syndrome, exhibits learning and behavioral
532 abnormalities. Proc Natl Acad Sci U S A *95*, 6256-6261.
533 Salehi, A., Delcroix, J.D., Belichenko, P.V., Zhan, K., Wu, C., Valletta, J.S., Takimoto-Kimura, R.,
534 Kleschevnikov, A.M., Sambamurti, K., Chung, P.P.*, et al.* (2006). Increased App expression in a mouse
535 model of Down's syndrome disrupts NGF transport and causes cholinergic neuron degeneration. Neuron
536 *51*, 29-42.
537 Tagawa, Y., Kanold, P.O., Majdan, M., and Shatz, C.J. (2005). Multiple periods of functional ocular
538 dominance plasticity in mouse visual cortex. Nat Neurosci *8*, 380-388.
539 Takashima, S., Becker, L.E., Armstrong, D.L., and Chan, F. (1981). Abnormal neuronal development in the
540 visual cortex of the human fetus and infant with down's syndrome. A quantitative and qualitative Golgi
541 study. Brain Res *225*, 1-21.

JNeurosci Accepted Manuscript

542 Tsai, L., and Barnea, G. (2014). A critical period defined by axon-targeting mechanisms in the murine
543 olfactory bulb. Science *344*, 197-200.
544 van Splunder, J., Stilma, J.S., Bernsen, R.M., Arentz, T.G., and Evenhuis, H.M. (2003). Refractive errors
545 and visual impairment in 900 adults with intellectual disabilities in the Netherlands. Acta Ophthalmol
546 Scand *81*, 123-129.
547 Vassar, R., Chao, S.K., Sitcheran, R., Nunez, J.M., Vosshall, L.B., and Axel, R. (1994). Topographic
548 organization of sensory projections to the olfactory bulb. Cell *79*, 981-991.
549 William, C.M., Andermann, M.L., Goldey, G.J., Roumis, D.K., Reid, R.C., Shatz, C.J., Albers, M.W., Frosch,
550 M.P., and Hyman, B.T. (2012). Synaptic plasticity defect following visual deprivation in Alzheimer's
551 disease model transgenic mice. J Neurosci *32*, 8004-8011.
552 Ye, Q., and Miao, Q.L. (2013). Experience-dependent development of perineuronal nets and chondroitin
553 sulfate proteoglycan receptors in mouse visual cortex. Matrix Biol *32*, 352-363.
554 Yu, C.R., Power, J., Barnea, G., O'Donnell, S., Brown, H.E., Osborne, J., Axel, R., and Gogos, J.A. (2004).
555 Spontaneous neural activity is required for the establishment and maintenance of the olfactory sensory
556 map. Neuron *42*, 553-566.
557 Yu, T., Liu, C., Belichenko, P., Clapcote, S.J., Li, S., Pao, A., Kleschevnikov, A., Bechard, A.R., Asrar, S.,
558 Chen, R.*, et al.* (2010). Effects of individual segmental trisomies of human chromosome 21 syntenic
559 regions on hippocampal long-term potentiation and cognitive behaviors in mice. Brain Res *1366*, 162-
560 171.
561 Zheng, H., Jiang, M., Trumbauer, M.E., Sirinathsinghji, D.J., Hopkins, R., Smith, D.W., Heavens, R.P.,
562 Dawson, G.R., Boyce, S., Conner, M.W.*, et al.* (1995). beta-Amyloid precursor protein-deficient mice
563 show reactive gliosis and decreased locomotor activity. Cell *81*, 525-531.
564 Zou, D.J., Feinstein, P., Rivers, A.L., Mathews, G.A., Kim, A., Greer, C.A., Mombaerts, P., and Firestein, S.
565 (2004). Postnatal refinement of peripheral olfactory projections. Science *304*, 1976-1979.

566

567

JNeurosci Accepted Manuscript

Figure 1. Defect in monocular deprivation-induced expansion of non-deprived eye response territory in Ts65Dn mice. *A–D*, Coronal sections of visual cortex demonstrating the pattern of *Arc* mRNA induction following stimulation of the ipsilateral eye in non-trisomic (A and C) and Ts65Dn (B and D) mice. In normally-reared mice, non-trisomic (A) and Ts65Dn (B) responses are similar. Following a 4-6 day period (from P27-29 to P31-P35) of monocular deprivation (MD), non-trisomic mice demonstrate the expected expansion in width of the domain responsive to the non-deprived eye (C). Ts65Dn mice do not demonstrate this expansion (D). E, Quantitation of results. Arrowheads denote medial and lateral edges of responsive domains. Cortical layers are labeled in B. Error bars denote standard deviation. Scale bar=500 μm; ***$p<1.24 \times 10^{-6}$, n.s.= not significant, *t*-test. Two-way ANOVA for interaction between genotype and MD, $p<0.0001$.

Figure 2. Defect in OD response shift following MD in Ts65Dn mice. *A*, Optical imaging schematic. *B*, Quantitation of responses. Following monocular deprivation (MD), non-trisomic (black) and Ts65Dn (red) mice demonstrate weakening of responses to the deprived, contralateral (contra) eye, however, only non-trisomic mice demonstrate strengthening of responses to the non-deprived, ipsilateral (ipsi) eye. # p=0.072, * p= 0.013, ***p= 0.00034. *C and D,* Shifts in ocular dominance index ODI (contra – ipsi/ contra + ipsi), for individual mice (C) and the averages for each group (D) demonstrate that the expected shift that occurs in non-trisomic mice is less robust in Ts65Dn mice. Error bars denote standard error. # p=0.06, * p=0.024, *** $p=4.44 \times 10^{-5}$, *t*-test.

Figure 3. Histologic assessment of neuronal populations in the Ts65Dn visual cortex. Representative immunostains (A-L) and Wisteria Floribunda Agglutinin (WFA) staining (M-O) of non-trisomic littermate (A,D,G,J,M) and Ts65Dn (B,E,H,K,N) visual cortex. No significant differences were observed in the density of $NeuN^+$ (A-C), $Gad67^+$ (D-F), $Parvalbumin^+$ (G-I), $Somatostatin^+$ (J-L) or WFA-stained neurons in Ts65Dn and non-trisomic visual cortex. C,F,I,L,O, quantitation of cell counts in non-trisomic (black) and Ts65Dn (red) cortex. Scale bar= 500 μm. Error bars denote standard deviation. n=6 per group.

JNeurosci Accepted Manuscript

Figure 4. Restoration of APP copy number in Ts65Dn mice fails to rescue OD plasticity defect. A. Following MD, Ts65Dn; APP2N mice demonstrate weakening of responses to the deprived eye (contra), but fail to demonstrate strengthening of responses to the non-deprived eye (ipsi). B. Plots of the ODIs of individual Ts65Dn; APP2N mice (n=11). Error bars denote standard error. *** $p=6.03 \times 10^{-5}$, t-test.

Figure 5. OD plasticity defect in Ts1Rhr mice. Similar to Ts65Dn mice, Ts1Rhr mice demonstrate a defect in OD plasticity by *Arc* induction (*A-E*) and optical imaging (*F-H*) assays. The expansion in the width of responsive cortex ipsilateral to the non-deprived eye that occurs in non-trisomic mice (*C*) does not occur in Ts1Rhr mice (*D*). Scale bar=500 μm. *E*, Quantitation of *Arc* data. ***$p=1.86 \times 10^{-7}$, t-test. *F,* Following MD, Ts1Rhr mice demonstrate weakening of responses to the non-deprived (ipsi) eye, instead of strengthening. * $p<0.048$ t-test. *G and H,* ODI shifts in Ts1Rhr mice are much less robust and driven entirely by weakening of responses to the deprived eye. * p=0.0237, two-way ANOVA.

Figure 6. Ts65Dn mice demonstrate a defect in olfactory glomerular refinement. Refinement of glomerular targeting was assessed in Ts65Dn (A-C) and Ts1Rhr (D-F) mouse models at P34-36. Ts65Dn mice (B) demonstrate impairment in refinement of connections to single glomeruli when compared to littermate controls (A). C, Quantitation of results in non-trisomic mice, Ts65Dn mice and Ts65Dn mice with 2 copies of APP (Ts65Dn;APP2N). 14 hemibulbs from 6 non-trisomic mice, 26 hemibulbs from 7 Ts65Dn mice and 13 hemibulbs from 4 Ts65Dn; APP2N mice were analyzed. Ts1Rhr mice (E) and littermate controls (D) demonstrate similar degrees of target refinement at P34-36 (p=0.86; quantitation in F). 14 hemibulbs from 4 non-trisomic mice and 18 hemibulbs from 5 Ts1Rhr mice were analyzed. Scale bar= 200 μm; * p=0.027, t-test.

Table 1. This table summarizes the results of assessments of OD plasticity and of olfactory glomerular refinement in mouse strains expressing mutant (Swedish mutation K670N, M671L; APPswe) or wildtype alleles of human APP and in Down syndrome model mice trisomic (Ts65Dn) or disomic (Ts65Dn; APP2N and Ts1Rhr) for APP. References to published data are cited.

JNeurosci Accepted Manuscript

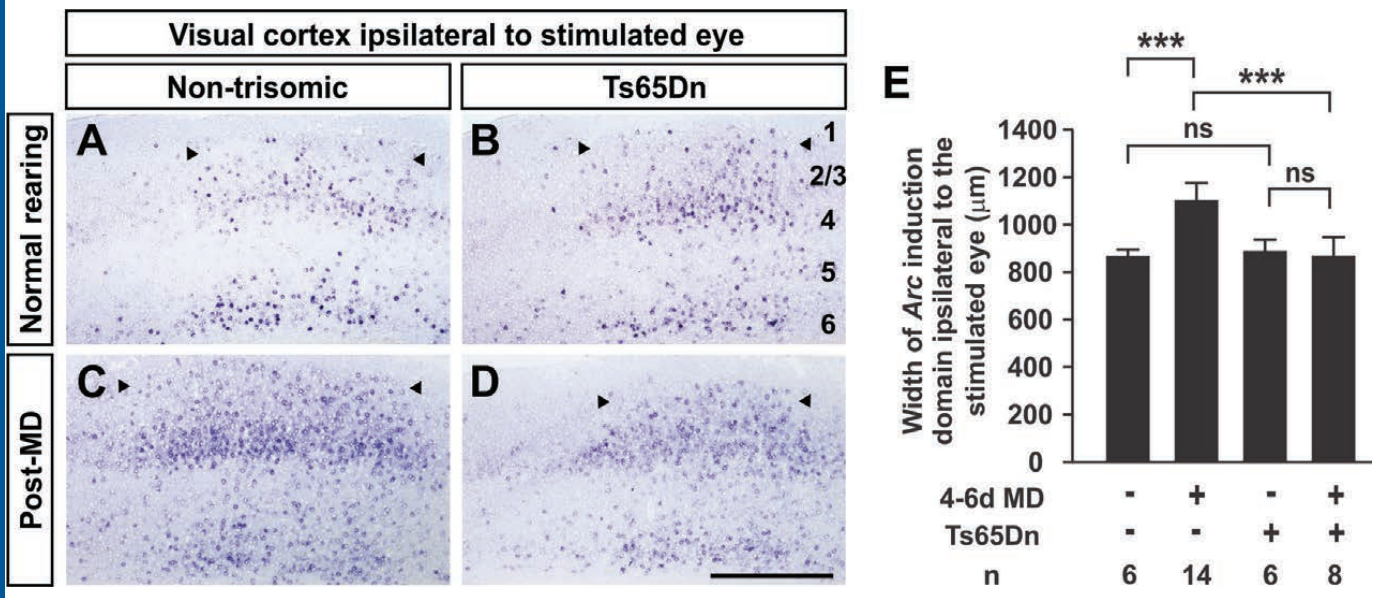

JNeurosci Accepted Manuscript

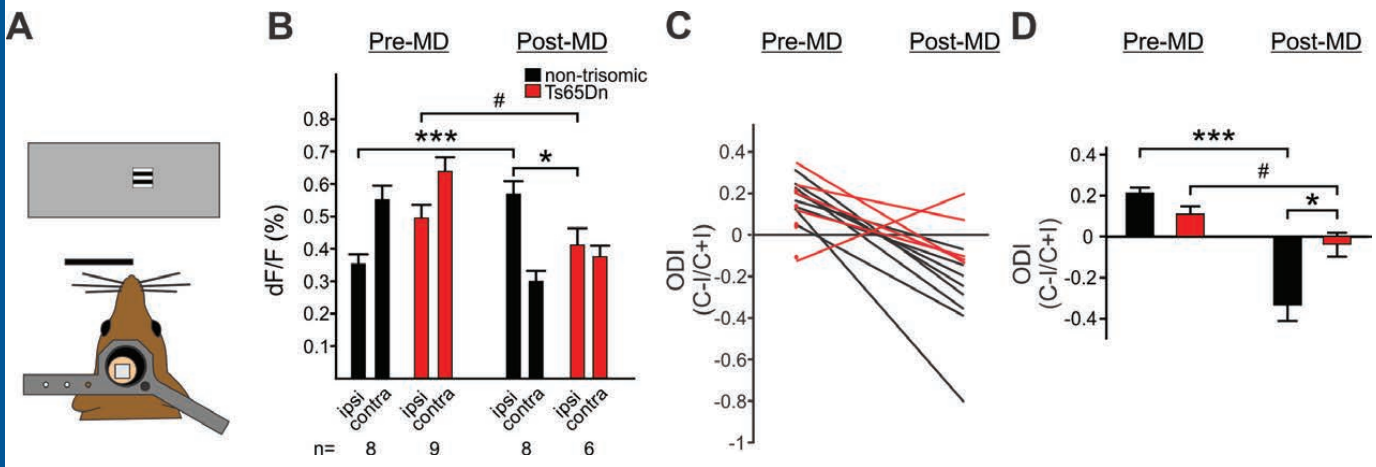

JNeurosci Accepted Manuscript

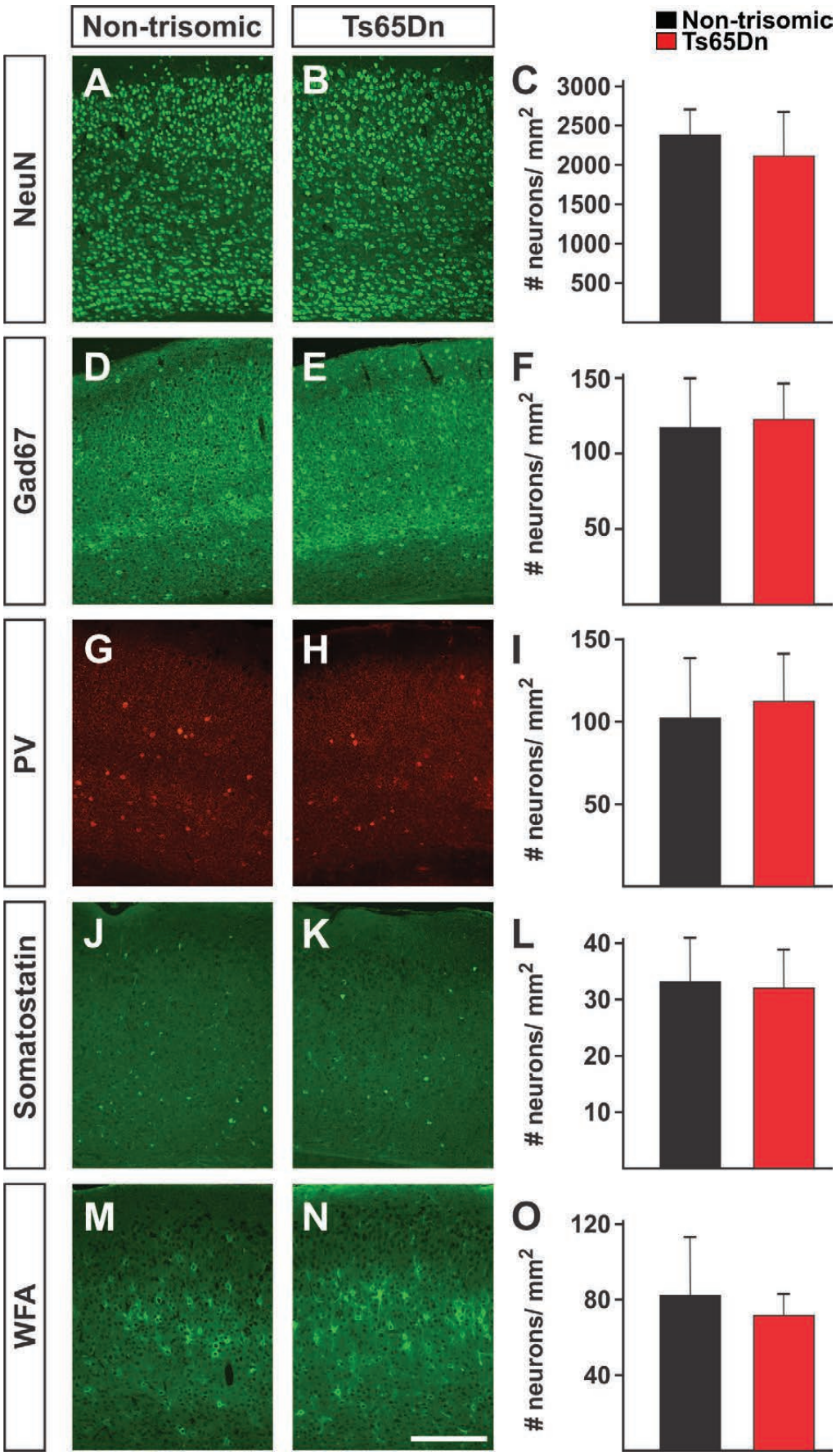

JNeurosci Accepted Manuscript

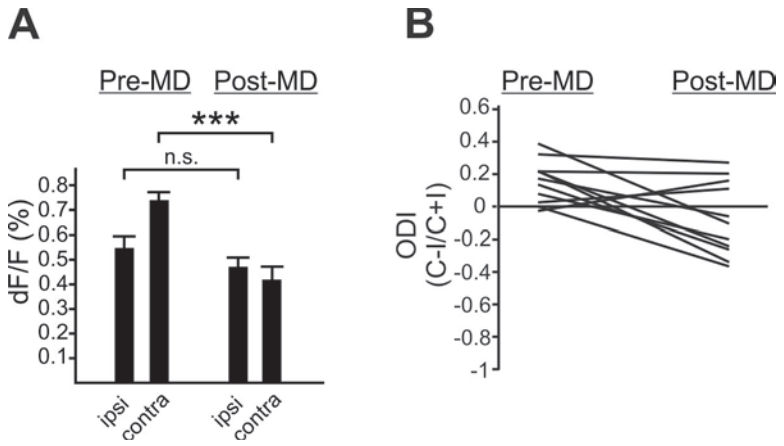

JNeurosci Accepted Manuscript

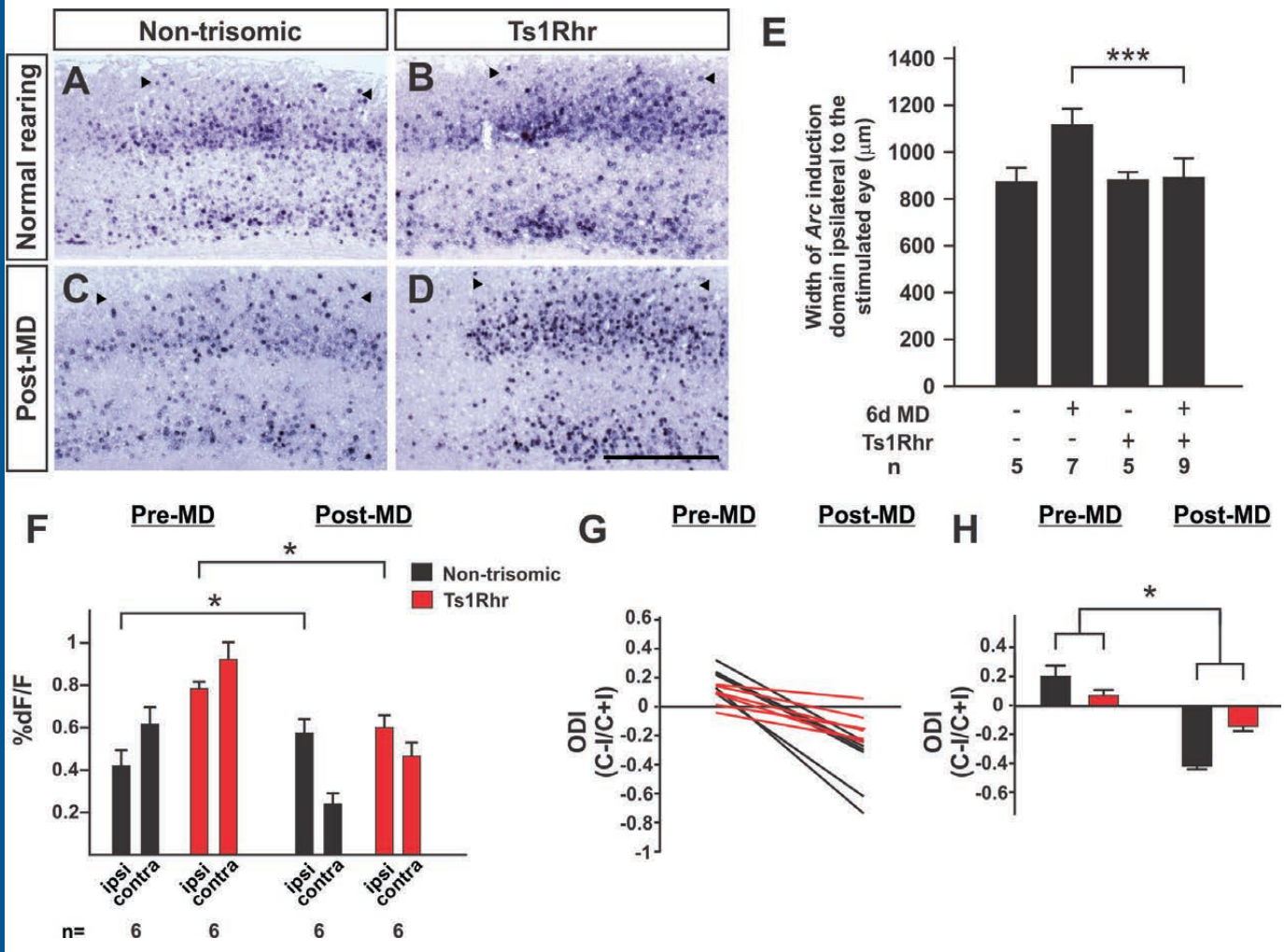

JNeurosci Accepted Manuscript

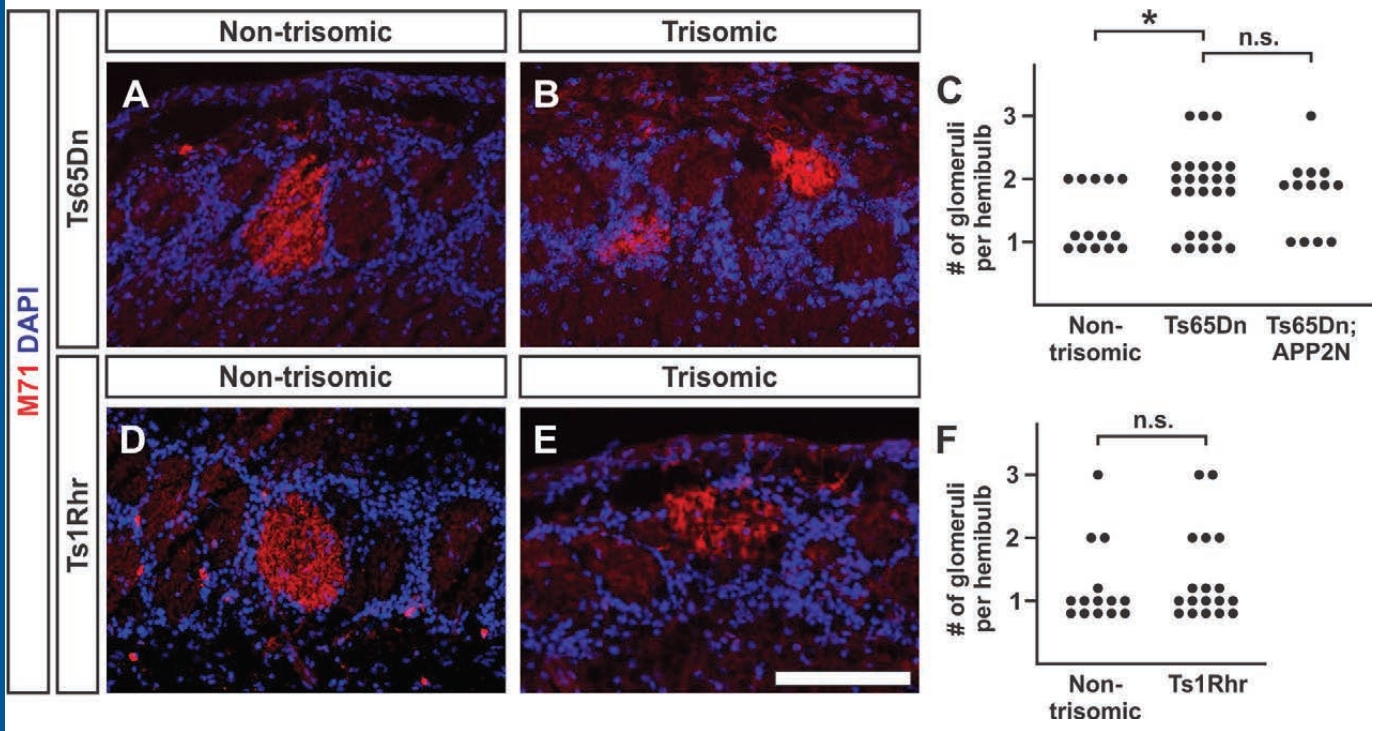

JNeurosci Accepted Manuscript

Table 1. Comparison of visual cortical plasticity and olfactory glomerular refinement phenotypes in mouse models of Alzheimer's disease and Down syndrome.

Genotype	Ocular dominance plasticity	Olfactory glomerular refinement
APPswe	Impaired (William et al., 2012)	Impaired (Cao et al., 2012)
Wild type human APP overexpression	Not tested	Normal (Cao et al., 2012)
Ts65Dn	Impaired	Impaired
Ts65Dn; APP2N	Impaired	Impaired
Ts1Rhr	Impaired	Normal